



A fully automated methodology for differentiating rock from snow, clouds and sea in Antarctica from Landsat imagery: A new rock outcrop map and area estimation for the entire Antarctic continent

Alex Burton-Johnson^{1*}, Martin Black^{1,2}, Peter T. Fretwell¹ and Joseph Kaluza-Gilbert³

5 ¹ British Antarctic Survey, Cambridge, CB3 0ET, UK

² Department of Geography, Environment and Earth Sciences, University of Hull, Hull, HU6 7RX, UK

³ School of Geography, Earth and Environmental Sciences, University of Birmingham, Birmingham, B15 2TT, UK

Correspondence to: Alex Burton-Johnson (alerto@bas.ac.uk)

Abstract. Differentiating exposed rock from snow and ice is a particular problem in Antarctica where extensive cloud cover
10 and widespread shaded regions lead to classification errors. The existing rock outcrop dataset has significant georeferencing
issues including overestimation and generalisation of rock exposure areas. The most commonly used method for automated
rock and snow differentiation, the Normalised Difference Snow Index (NDSI), has difficulty differentiating rock and snow in
Antarctica due to misclassification of shaded pixels and cannot differentiate illuminated rock from clouds. This study presents
15 a new method for identifying rock exposures using Landsat 8 data. This is the first fully automated methodology for snow and
rock differentiation that excludes areas of snow (both illuminated and shaded), clouds and liquid water whilst identifying both
sunlit and shaded rock, achieving higher and more consistent accuracies than alternative data and methods such as the NDSI.
The new methodology has been applied to the whole Antarctic continent (north of 82°40' S) using Landsat 8 data to produce
a new rock outcrop dataset for Antarctica. The new data (merged with existing data south of 82°40' S) reveals that exposed
rock forms 0.18% of the total land area of Antarctica; half of previous estimates.

20 1 Introduction

Differentiating areas of snow and exposed rock in Antarctica is important in a variety of contexts, including mapping,
navigation, glaciological, geological and geomorphological research, and monitoring changes in the ice sheet and its response
to climate change. The only existing continent-wide geospatial dataset for exposed rock in Antarctica is available from the
Scientific Committee on Antarctic Research (SCAR) Antarctic Digital Database (ADD) website, www.add.scar.org. This data
25 (the ADD rock outcrop dataset) has been derived through manual identification and digitization of published topographic
maps. This data comes from a variety of sources and variety of scales and accuracies, so the quality of the dataset is regionally
inconsistent and has no quality assessment associated with it (in contrast to the automated identification method presented here
for which accuracies and error sources have been determined). Although extensively used (over 2500 downloads of the rock
dataset in the last 3 years) the data suffers from poor georeferencing, frequent misclassification of shaded snow as rock, as



well as overestimating and generalising areas of rock exposure. Additionally as satellite derived coastlines and digital elevation models become available, the inconsistency and inaccuracy of the present cartographically derived ADD rock outcrop dataset becomes difficult to resolve with these new data sources. There is therefore an urgent need to improve the consistency georeferencing and accuracy of rock outcrop data for Antarctica.

5 In several temperate regions methods have been formulated to automatically identify exposed rock outcrop from satellite imagery (e.g. Racoviteanu *et al.* 2010, Dozier 1989, Hall *et al.* 1995, Paul *et al.* 2002, Paul *et al.* 2009, Bolch *et al.* 2010, Zhu & Woodcock 2012, Zhu *et al.* 2015), but the methods have never been applied to Antarctica. The most commonly used existing method for delineating snow cover and rock outcrop is the Normalised Difference Snow Index (NDSI, Hall *et al.* 1995, Dozier
10 1989). The NDSI was developed following other indices, such as the Normalised Difference Vegetation Index (NDVI, Tucker 1986, Tucker 1979), initially for application to MODIS and Landsat satellite imagery. The NDSI is calculated according to equation (1) (modified for Landsat 8 data) where Landsat 8 band 3 equates to spectral wavelengths of 0.53 to 0.59 μm (the green band) and Landsat 8 band 6 equates to spectral wavelengths of 1.57 to 1.65 μm (the short wavelength infrared band, SWIR 1):

$$NDSI = \frac{\text{Landsat 8 band 3} - \text{Landsat 8 band 6}}{\text{Landsat 8 band 3} + \text{Landsat 8 band 6}} \quad (1)$$

15 Equation (1) works on the basis that snow reflects visible wavelengths more strongly than middle-infrared wavelengths whilst rock displays a slightly higher reflectance for middle infrared wavelengths than visible wavelengths (Fig. 1) and so a threshold value can be determined for the NDSI of an image differentiating pixels of snow and rock (typically in the range 0.25 to 0.45 - Hall *et al.*, 1995). One problem for application of the thresholded NDSI technique to automated snow and rock differentiation is that the optimal threshold value must be determined for each individual image being analysed or even within the same image
20 due to changes in illumination or fresh snow cover across the image's area (Burns and Nolin, 2014). It is often the case that the optimal threshold is manually determined on each scene by comparison to reference data, however this becomes a problem when large numbers of images need to be analysed or reference data is not available.

Although the application of the NDSI has been successful at lower latitudes (e.g. Burns & Nolin 2014) where vertically illuminated imagery is available, high solar elevation angles in Antarctica lead to exclusion of shaded rock. This issue of
25 shaded rock is greater in Antarctica where unavoidably low sun angle results in large percentages of the outcrop being in shadow. The problem has been addressed for glacier mapping at lower latitudes by thresholding the Landsat blue band (in addition to an NDSI or alternative band ratio threshold) due to the higher reflectance of shaded snow than shaded rock in blue wavelengths (Arendt *et al.*, 2012; Bishop *et al.*, 2004; Paul *et al.*, 2007; Paul and Käab, 2005).

Unavoidable cloud cover in some Antarctic images, especially on the Antarctic Peninsula, leads to the classification of clouds
30 as rock exposure by the NDSI technique (Fig. 2) as the two are indiscernible using this methodology. Any effective dataset of rock outcrop in Antarctica would have to ensure that clouds are not misrepresented.

A further problem for automated rock identification at lower latitudes is debris cover on glaciers which is indiscernible in multispectral imagery from exposed rock (Paul *et al.*, 2004). This is accentuated by the melting and ablation of low latitude



glaciers (Stokes et al., 2007) and is intensified by large amount of debris from frost shattering and freeze thaw activity (Fig. 3a and 3b). However Antarctic glaciers are rarely debris covered due the prevailing climatic conditions where constant sub-freezing conditions result in a lack of ablation (Fig. 3c and 3d) . The limited number of positive degree days and the lack of a day/night cycle at polar latitudes reduces freeze thaw activity meaning that less frost shattering takes place. Most Antarctic glaciers and ice streams are marine terminating and relatively few have active ablation zones (with the exception of a small percentage on the northern and eastern Antarctic Peninsula. The result is that most Antarctic glaciers are largely debris-free, removing this limitation from our study.

Here we present a new technique for fully automated rock outcrop identification using freely available Landsat satellite data. The method is a composite technique combining separate algorithms that divide the image into cloud, liquid water, shaded snow and sunlit snow and shaded and sunlit rock exposures. We test the method against manually digitised polygons, the existing ADD rock outcrop dataset and the NDSI to validate and compare its accuracy.

We apply the new methodology to the entire landmass of Antarctica, (>12,000,000 km²) using Landsat 8 data over all regions of the continent that contain rock outcrop. The resulting dataset represents an improvement over the previous dataset (ADD), providing consistent and accurate estimation of the amount and location of rock outcrop in Antarctica.

2. New Methodology

2.1 Input data

To produce a rock outcrop map for the entire Antarctic continent requires a freely available georeferenced multiband dataset. The dataset must cover high latitudes; be recently acquired; be of a high enough resolution to identify individual outcrops and geomorphological features; and individual images must have a large enough extent for manual selection of suitable tiles for the entire continent. On this basis, the Landsat 8 multispectral satellite data was chosen for analysis. Landsat 8 is the latest and continuing satellite mission for multispectral global data acquisition launched by NASA and the United States Geological Survey (Roy et al., 2014). The satellite's sensors record 8 electromagnetic bands (0.43 to 2.29 μm wavelengths) at 30m resolution, plus a panchromatic band (0.50 to 0.68 μm) at 15m resolution and two thermal infrared bands (TIRS 1 and 2, 10.60 to 12.51 μm) acquired at 100m resolution and resampled to 30m.

For the production of an Antarctic-wide rock outcrop map, tiles were selected that were acquired during the Austral summer and display strong illumination and minimal cloud cover. Of particular importance was to exclude tiles with extensive cumulus or stratocumulus cloud where shadows within and below the cloud layer can be indiscernible from illuminated rock exposure. A total of 249 Landsat 8 tiles meeting these requirements were identified using the USGS Earth Explorer website (earthexplorer.usgs.gov). Details of the tiles used are provided as supplementary material.

In addition to the raw data, pre-processed tiles (170 km North-South by 183 km East-West) corrected for top of atmosphere reflectance, surface reflectance and brightness temperature are freely available for download (espa.cr.usgs.gov). However, the calculation of surface reflectance values in Antarctica is problematic due to a lack of adequate atmospheric correction models



for the continent, limited *in situ* atmospheric data and inadequate quality elevation data (Black et al., 2014). This renders the surface reflectance corrected data unsuitable and so top of atmosphere reflectance and brightness temperature corrected products were used instead for this study.

2.2 Methodology

5 The new methodology identifies areas of sunlit and shaded rock through two separate workflows and then merges both outputs to produce the final dataset. Within both procedures a series of masks are produced to identify areas of exposed outcrop and to exclude areas of snow, cloud and liquid water. At each stage band ratios were used in preference to threshold values for individual bands to allow application of a single set of threshold values to a large dataset. These two procedures are detailed below and a flowchart for executing this process shown in Fig. 4. The complete methodology was automated within ArcPy
10 (Zandbergen, 2013). The script is included in the supplementary material.

Procedure A. Sunlit Rock:

A.1. Sunlit rock identification: the NDSI

Although the NDSI is unable to identify shaded rock and often misclassifies clouds as rock outcrop, it remains the best method for identifying regions of exposed sunlit rock. Consequently, it is the primary input for this methodology with a threshold
15 value of <0.75 being used to identify pixels of sunlit rock outcrop and confidently exclude pixels of snow (Fig. 5a).

A.2. Cloud mask: TIRS / Blue and TIRS1 Threshold

One of the main problems of rock outcrop identification in Antarctica is that sunlit rock and clouds are indiscernible using the NDSI alone (Fig. 5a). Consequently we have derived a mask for sunlit snow and clouds using the thermal infrared band (TIRS1, 10.60 to 11.19 μm) and the blue band. Using a ratio of these bands, clouds and sunlit snow give low values as they
20 are cold but have high blue reflectance (Fig. 5b). In contrast, pixels of sunlit and shaded rock are warmer when associated with high blue reflectance or colder when associated with low blue reflectance, resulting in high to moderate ratio values. However, shaded snow and liquid water also give high to moderate values. A TIRS/blue threshold value of >0.4 is most effective in selecting cloud free pixels and excluding pixels of sunlit snow and cloud to produce an accurate final product, although some sunlit rock pixels are also discarded (Fig. 5b). To aid this cloud masking further an absolute TIRS1 threshold of >2550 is also
25 applied as $<1\%$ of sunlit rock pixels have lower TIRS1 values whilst 10% of cloud pixels and 5% of sunlit and shaded snow pixels do have lower values (Fig. 5c).

A.3. Liquid water mask: NDWI and coastline

The most widely applied approach for the identification of liquid water in multispectral imagery is the Normalised Difference Water Index (NDWI, McFeeters 1996). Modified for Landsat 8 data with Landsat 8 band 3 equating to spectral wavelengths



of 0.53 to 0.59 μm (the green band) and Landsat 8 band 5 equating to spectral wavelengths of 0.85 to 0.88 μm (the near infrared band, NIR) the NDWI is calculated using equation (2):

$$NDWI = \frac{\text{Landsat 8 band 3} - \text{Landsat 8 band 5}}{\text{Landsat 8 band 3} + \text{Landsat 8 band 5}} \quad (2)$$

A liquid water mask is applied to both the sunlit and shaded rock identification procedures, and so the same threshold value of <0.45 is used for both (Fig. 5d). Unfortunately, due to the presence of calved ice and suspended glacial debris in Antarctic coastal seawater, a large overlap in NDWI values exists between pixels of sea and shaded rock exposure (Fig. 5d). To aid this step the manually derived coastline of Antarctica (available from www.add.scar.org) was also used as a mask for excluding liquid water and sea ice.

Procedure B. Shaded Rock:

10 B.1. Shaded rock identification: Blue threshold

Even in the shade, snow is more reflective at blue wavelengths than shaded rock. Consequently by determining the blue intensity values for a pixels representing rock and snow a threshold value of <2500 was found to successfully identify pixels containing shaded rock exposure.

B.2. Liquid water mask: NDWI and coastline

15 Although a blue wavelength threshold successfully differentiates shaded snow and rock, liquid water is also misclassified as rock. Thus, the NDWI and coastline mask applied to the sunlit rock data are also applied to the shaded rock data (again using the NDWI threshold value of <0.45, Fig. 5d). This step also aids exclusion of shaded snow pixels as 25% of their values are discarded by the NDWI threshold (Fig. 5d).

Procedure C. Applying the masks and merging the datasets

20 Pixels that were identified as rock by the NDSI mask and not identified as cloud or water represent sunlit rock outcrops. Similarly, pixels with blue band intensities below the threshold for shaded rock that aren't subsequently identified as liquid water by the NDWI threshold represent shaded rock exposures. Merging these two outputs produced the rock outcrop map for each tile. The output of each tile was then reprojected to the same coordinate system and the results of all tiles mosaicked together for the entire continent. As most areas were covered by multiple Landsat tiles, any pixels identified as rock exposure
25 by any of the overlying tiles was included as exposed rock in the final dataset. Finally, this dataset was merged with the existing ADD rock outcrop dataset for areas not covered by the LANDSAT 8 imagery (Fig. 6).



3. Results

3.1 Accuracy Assessment

To quantify the accuracy of the new methodology and its limitations, the extent of rock exposure was manually delineated using ten 10x10 km images (110,889 pixels each, Fig. 7). Images were selected from distal locations across the continent (Fig. 8), covering a range in geology, geomorphology and latitude. Areas of rock outcrop were manually identified by three operators. One tile (Ryder Bay, Fig. 7a) was traced by all operators; operator variability for pixel identification (rock or non-rock) was $\pm 0.27\%$ (one standard deviation).

The manually derived land cover was compared with the existing ADD rock outcrop dataset, the new automated method and the optimum NDSI-determined output for each image. Optimum NDSI threshold values (maximum values for pixels identified as rock) were taken as those with the lowest total quantity disagreement (abundance accuracy) and allocation disagreement (location accuracy) (Pontius Jr&Millones 2011). As shown by Fig. 9, optimum NDSI threshold values are highly variable. For well illuminated images without any cloud cover (Fig. 7b to 7f), NDSI threshold values of 0.6 or 0.7 are optimal. Images of extensive shade achieve more accurate results at higher NDSI threshold values (0.8, Fig. 7g) allowing identification of shaded rock. In contrast, images with extensive cloud require lower values (0.3 to 0.5, Fig. 7a, h and i) so as not to include the cloud as misidentified rock outcrop pixels. For mixed images (Fig. 7j) with shaded and illuminated rock with minor cloud cover, 0.7 remained the optimal threshold value.

Well illuminated, cloud free images produce similar accuracies for the NDSI techniques and the new method (Fig. 7b to 7f), with low commission or omission disagreements (Fig. 10a). However, the required determination of an optimal NDSI threshold value renders this alternative methodology more involved than that used for our new dataset;, when using the optimal threshold value the NDSI technique omits areas of rock in shaded images as well as both shaded or sunlit rock in cloudy images, leading to high and variable omission disagreements (Fig. 10b).

The ADD rock outcrop dataset produces variable accuracies. In Ryder Bay (Fig. 7a) the map has been recently been updated using manual delineation from very high resolution aerial photography and so has high accuracy with low omission and commission disagreement, similar to the new dataset. However, it is important to stress that areas of high resolution delineation are limited in the ADD rock outcrop dataset. The ADD rock outcrop dataset is more accurate than the NDSI technique in shaded images (Fig. 7g and 7j), but highly generalised and poorly georeferenced outcrop extents in other tiles (Fig. 7e and 7h) produce high and highly variable disagreements (Fig. 10), particularly in commission.

The new methodology performed poorest in images with limited areas of rock outcrop (e.g. Fig. 7h, 0.1% rock), although shade, clouds and mixed pixels of snow and rock in Fig. 7h make even manual pixel identification difficult. There are omission disagreements in shaded images (Fig. 7g and 7j) although these are much lower than for the alternative techniques (a mean of 15% for all images compared to 38% for the NDSI technique and 30 % for the ADD rock outcrop dataset, Fig. 10b). Clouds were successfully masked and do not contribute to the commission disagreement (Fig. 7h, i and j). The quality assessment shows higher accuracies for the new method (a mean of $85 \pm 8\%$ of identified rock pixels being correct for all ten images



compared with $62 \pm 32\%$ or $70 \pm 14\%$ for the NDSI technique and ADD rock outcrop dataset respectively) with lower and much more consistent commission and omission disagreements than the alternative NDSI or ADD rock outcrop datasets (Fig. 10b).

4. Discussion

- 5 This is the first fully automated methodology for the differentiation of snow and rock in Antarctica, from which a new outcrop map of the entire Antarctic continent has been produced at higher and more consistent accuracies than existing data and techniques ($85 \pm 8\%$ mean correct pixel identification for the new method compared to $62 \pm 32\%$ or $70 \pm 14\%$ for the NDSI and ADD data respectively, Fig. 10). The new dataset is available online via the SCAR ADD website (www.add.scar.org) and from this article's supplementary material.
- 10 Despite the poorer accuracy of the ADD rock outcrop dataset (70% mean for correct pixel identification compared to 85% for the new dataset), due to the methodology by which it was derived, certain features are better represented. This includes South Georgia and the South Orkney Islands where a lack of cloud-free imagery in the late Austral summer (when the outcrops aren't covered by snow) prevents automated outcrop identification. Consequently, rock outcrop extents in these areas are derived from the existing ADD dataset rather than remotes sensing imagery in addition to outcrops south of $82^{\circ}40'$ S (Fig. 6).
- 15 It is important when using the new Landsat 8 rock outcrop map to consider seasonal variability in snow cover and that most outcrops were derived from multiple tiles from different years and different months of the Austral summer. Consequently, the map may not be representative of current conditions and may not consistently represent maximum outcrop extent across the continent.

4.1 Limitations

- 20 Using the new methodology we have produced a revised map of rock outcrops in Antarctica. Landsat 8 does not provide coverage south of $82^{\circ}40'$ S so the existing ADD rock outcrop dataset was clipped to latitudes greater than this and merged with the new automatically derived data to produce the final dataset. There are two further limitations to the new methodology:
- 25 1. Because an overlap exists between the NDWI values of shaded rock and liquid water (Fig. 5d), some pixels of coastal seawater not masked by the ADD coastline have been misidentified as exposed rock. This is particularly problematic for pixels adjacent to seawater rich in calved ice and glacial debris (Fig. 11a). These pixels are spectrally identical to shaded rock and thus cannot be excluded automatically from the data. Consequently they were manually removed from the final dataset, although some of these misidentified pixels may still be present.
 - 30 2. Even though spectral properties have been chosen that distinguish rock pixels from those of snow, clouds or sea, some overlap exists where pixels remain ambiguous (Fig. 5). Consequently, to allow automated analysis over such a large area mildly conservative threshold values were chosen. For example, the NDSI threshold for sunlit rock set at the 95th percentile rather than the complete range exhibited by sunlit outcrops as this excludes any overlap with the range of NDSI values for



sunlit snow (Fig. 5a). This results in the exclusion of some pixels of exposed rock that are spectrally similar to clouds and snow (e.g. Fig. 11b).

3. Due to the 100m spatial resolution of the TIRS band, small outcrops around the continent (especially those less than 60m or 2 pixels across) are often excluded by the new technique and may be better represented in the ADD rock outcrop dataset.

5 4.2 Total outcrop area

We calculate (using an Equal Area projection) that the existing ADD rock outcrop dataset has 44,900 km² area of rock outcrop, equivalent to 0.37% of the total land area of Antarctica (12,188,650 km²). In contrast the new data has a 21,745 km² total area of rock outcrop, equivalent to 0.18% of the continent's land area and 48% of the previous estimate. This is a significant decrease and highlights an overestimation in the current predictions of rock outcrop extent in Antarctica.

10 4.3 Applications and future developments

The new Landsat 8 rock outcrop map will provide a revised and accurate base dataset for future topographical, glaciological, geological and geomorphological mapping. A number of satellite programs collecting new high resolution colour images are currently under development or planned for launch, including Digitalglobe's Worldview-3 satellite, NASA's HypsIRI satellite, European Space Agency's Sentinel program and the continuing Landsat data acquisition; these new datasets will allow further application of this technique at higher resolutions and consequently higher accuracies, allowing future improvement of the datasets broader applications. Application of the new technique to these alternative datasets would however require modification of the threshold values for each mask in the procedure.

5. Conclusions

A new map of exposed rock outcrop has been developed for the Antarctic continent. The new map was achieved via a fully automated methodology employing Landsat 8 multispectral imagery. The new methodology uses the NDSI technique to identify sunlit rock exposure and low blue intensities for shaded rock, and then applies separate masks to remove incorrectly classified pixels of cloud, snow and liquid water. This is the first automated methodology for rock outcrop identification in Antarctica, and achieves higher and more consistent accuracies than the existing dataset or what can be achieved using the alternative automated technique (the NDSI). Assessing the accuracy of these alternative techniques and datasets across a range of images gives a mean value for correct pixel identification of 85 ± 8% for the new method compared to 62 ± 32% or 70 ± 14% for the NDSI technique and existing ADD rock outcrop dataset respectively. The new map, supplemented by existing data for latitudes south of 82°40' S (the limit of Landsat 8 coverage), reveals that rock outcrop forms 0.18% of the total land area of Antarctica, 48% of the previous estimate.



Acknowledgements

This study is part of the British Antarctic Survey Polar Science for Planet Earth programme, funded by the Natural Environment Research Council.

References

- 5 Arendt, A., Bolch, T., Cogley, J. G., Gardner, A., Hagen, J.-O., Hock, R., Kaser, G., Pfeffer, W. T., Moholdt, G., Paul, F. and others: Randolph glacier inventory [v2. 0]: A dataset of global glacier outlines. Global land ice measurements from space, boulder Colorado, USA, 2012.
- Baldrige, A. M., Hook, S. J., Grove, C. I. and Rivera, G.: The ASTER spectral library version 2.0, *Remote Sens. Environ.*, 113(4), 711–715, 2009.
- 10 Bishop, M. P., Olsenholler, J. A., Shroder, J. F., Barry, R. G., Raup, B. H., Bush, A. B., Copland, L., Dwyer, J. L., Fountain, A. G., Haeberli, W. and others: Global Land Ice Measurements from Space (GLIMS): remote sensing and GIS investigations of the Earth's cryosphere, *Geocarto Int.*, 19(2), 57–84, 2004.
- Black, M., Fleming, A., Riley, T., Ferrier, G., Fretwell, P., McFee, J., Achal, S. and Diaz, A. U.: On the Atmospheric Correction of Antarctic Airborne Hyperspectral Data, *Remote Sens.*, 6(5), 4498–4514, 2014.
- 15 Bolch, T., Menounos, B. and Wheate, R.: Landsat-based inventory of glaciers in western Canada, 1985–2005, *Remote Sens. Environ.*, 114(1), 127–137, 2010.
- Burns, P. and Nolin, A.: Using atmospherically-corrected Landsat imagery to measure glacier area change in the Cordillera Blanca, Peru from 1987 to 2010, *Remote Sens. Environ.*, 140, 165–178, 2014.
- Dozier, J.: Spectral signature of alpine snow cover from the Landsat Thematic Mapper, *Remote Sens. Environ.*, 28, 9–22, 20 1989.
- Hall, D. K., Riggs, G. A. and Salomonson, V. V.: Development of methods for mapping global snow cover using moderate resolution imaging spectroradiometer data, *Remote Sens. Environ.*, 54(2), 127–140, 1995.
- McFeeters, S. K.: The use of the Normalized Difference Water Index (NDWI) in the delineation of open water features, *Int. J. Remote Sens.*, 17(7), 1425–1432, 1996.
- 25 Paul, F. and Kääb, A.: Perspectives on the production of a glacier inventory from multispectral satellite data in Arctic Canada: Cumberland Peninsula, Baffin Island, *Ann. Glaciol.*, 42(1), 59–66, 2005.
- Paul, F., Kääb, A., Maisch, M., Kellenberger, T. and Haeberli, W.: The new remote-sensing-derived Swiss glacier inventory: I. Methods, *Ann. Glaciol.*, 34(1), 355–361, 2002.
- Paul, F., Huggel, C. and Kääb, A.: Combining satellite multispectral image data and a digital elevation model for mapping 30 debris-covered glaciers, *Remote Sens. Environ.*, 89(4), 510–518, 2004.
- Paul, F., Kääb, A. and Haeberli, W.: Recent glacier changes in the Alps observed by satellite: Consequences for future monitoring strategies, *Glob. Planet. Change*, 56(1), 111–122, 2007.



- Paul, F., Barry, R. G., Cogley, J. G., Frey, H., Haerberli, W., Ohmura, A., Ommanney, C. S. L., Raup, B., Rivera, A. and Zemp, M.: Recommendations for the compilation of glacier inventory data from digital sources, *Ann. Glaciol.*, 50(53), 119–126, 2009.
- Pontius Jr, R. G. and Millones, M.: Death to Kappa: birth of quantity disagreement and allocation disagreement for accuracy assessment, *Int. J. Remote Sens.*, 32(15), 4407–4429, 2011.
- 5 Racoviteanu, A. E., Paul, F., Raup, B., Khalsa, S. J. S. and Armstrong, R.: Challenges and recommendations in mapping of glacier parameters from space: results of the 2008 Global Land Ice Measurements from Space (GLIMS) workshop, Boulder, Colorado, USA, *Ann. Glaciol.*, 50(53), 53–69, 2010.
- Roy, D. P., Wulder, M. A., Loveland, T. R., Woodcock, C. E., Allen, R. G., Anderson, M. C., Helder, D., Irons, J. R., Johnson, D. M., Kennedy, R. and others: Landsat-8: Science and product vision for terrestrial global change research, *Remote Sens. Environ.*, 145, 154–172, 2014.
- 10 Stokes, C. R., Popovnin, V., Aleynikov, A., Gurney, S. D. and Shahgedanova, M.: Recent glacier retreat in the Caucasus Mountains, Russia, and associated increase in supraglacial debris cover and supra-/proglacial lake development, *Ann. Glaciol.*, 46(1), 195–203, 2007.
- 15 Tucker, C. J.: Red and photographic infrared linear combinations for monitoring vegetation, *Remote Sens. Environ.*, 8(2), 127–150, 1979.
- Tucker, C. J.: Cover Maximum normalized difference vegetation index images for sub-Saharan Africa for 1983–1985, *Int. J. Remote Sens.*, 7(11), 1383–1384, 1986.
- Zandbergen, P. A.: Python scripting for ArcGIS., 2013.
- 20 Zhu, Z. and Woodcock, C. E.: Object-based cloud and cloud shadow detection in Landsat imagery, *Remote Sens. Environ.*, 118, 83–94, 2012.
- Zhu, Z., Wang, S. and Woodcock, C. E.: Improvement and expansion of the Fmask algorithm: cloud, cloud shadow, and snow detection for Landsats 4–7, 8, and Sentinel 2 images, *Remote Sens. Environ.*, 159, 269–277, 2015.

25 Acknowledgements

This study is part of the British Antarctic Survey Polar Science for Planet Earth programme, funded by the Natural Environment Research Council.

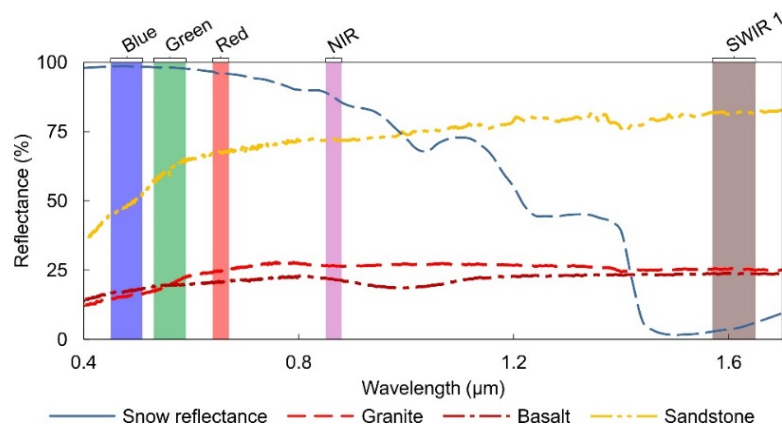


Fig. 1. Spectral reflectance data for snow and rock (granite, basalt and sandstone) from the ASTER Spectral Library v1.2 (Baldrige et al., 2009). Designations of spectral regions as defined by the Landsat 8 bands: Blue – Band 2, 0.45 – 0.51 μm ; Green – Band 3, 0.53 – 0.59 μm ; Red – Band 4, 0.64 – 0.67 μm ; NIR, Near Infrared – Band 5, 0.85 – 0.88 μm ; SWIR 1, Short Wave Infrared – Band 6, 1.57 – 1.65 μm .

5

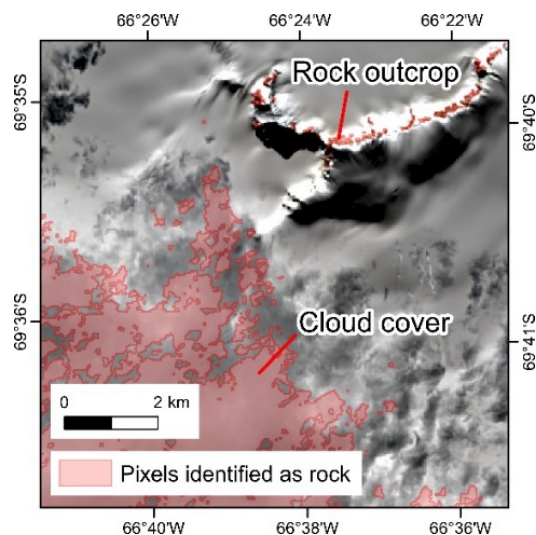


Fig. 2. Illustration of the misclassification of cloud cover as rock pixels when using the NDSI technique. An NDSI threshold of 0.6 was used to identify the rock outcrops, but at this threshold much of the cloud cover is also included.

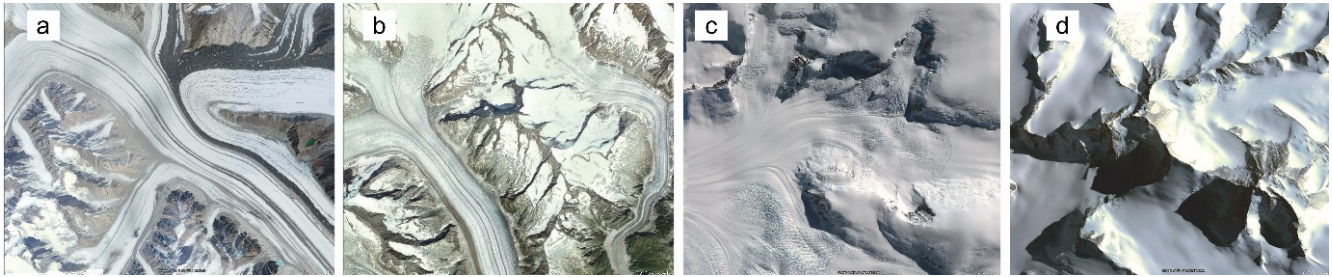


Fig. 3. Comparison of debris cover for glaciers at low latitudes (3a, Karakoram Range (35°N), and 3b, Jungfrau Range, Alps (46°N)) with those of Antarctica (3c, Antarctic Peninsula (66°S), and 3d, Transantarctic Mountains (72°S)). Note the lack of surface moraine and the deep shadows in 3e and 3d, typical of Antarctic glaciers where a lack of day-night cycle and year-round low temperatures restricts freeze thaw action and the permanently low sun angles result in deep shadows in remotely sensed imagery.

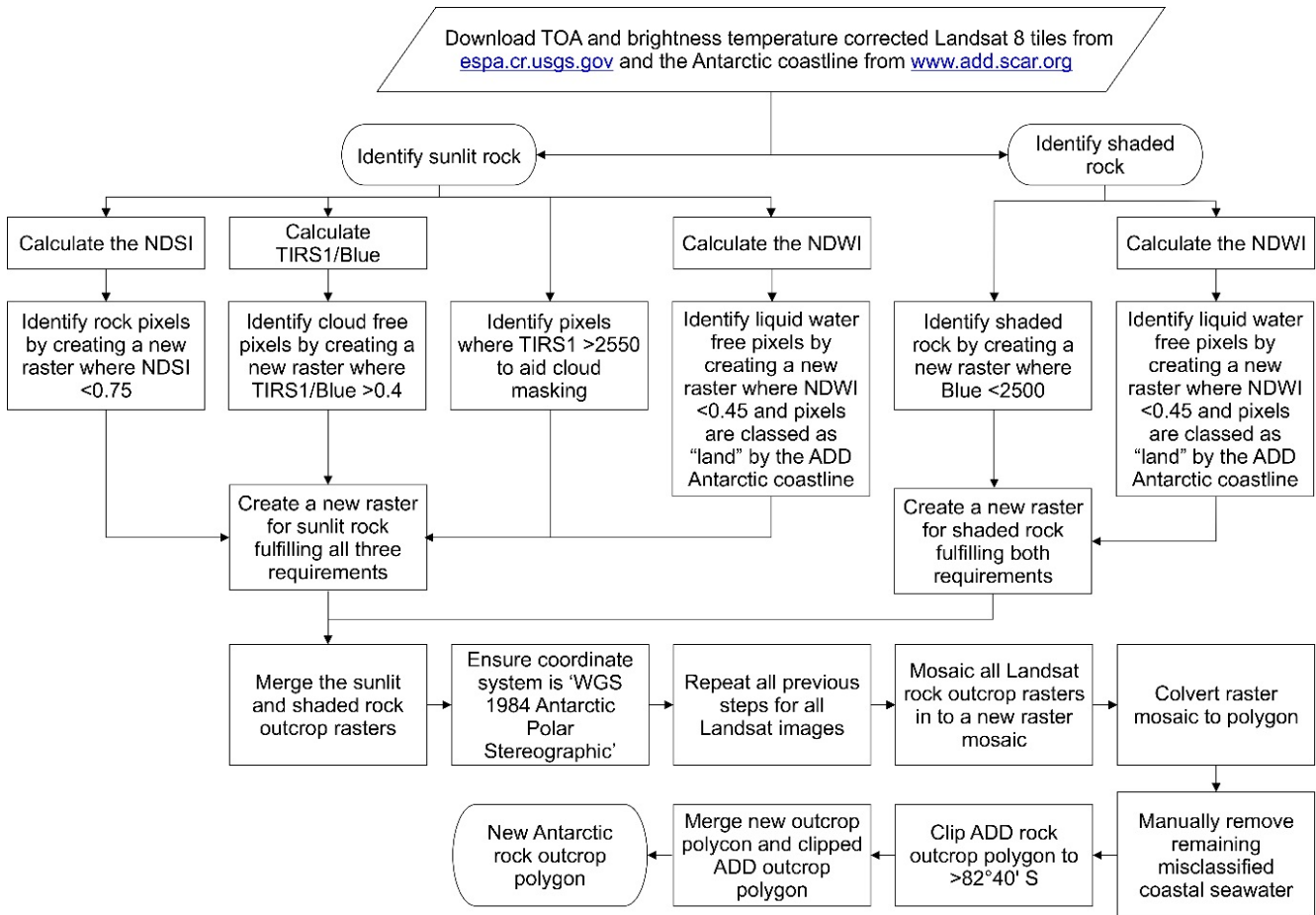


Fig. 4. Flowchart for the automated identification of rock outcrops in Antarctica using the new methodology.

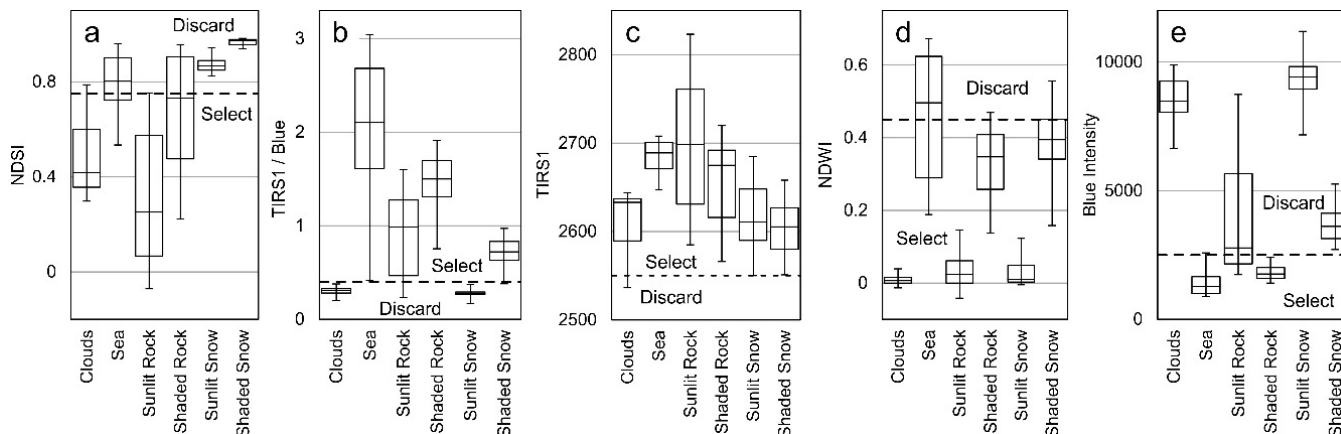


Fig. 5. Box plots of extracted pixel values from three Landsat 8 tiles illustrating the different spectral properties of clouds ($n = 871$), sea ($n = 3277$), sunlit rock ($n = 1158$), shaded rock ($n = 1224$), sunlit snow ($n = 1293$) and shaded snow ($n = 918$). Boxes indicate the 2nd and 3rd quartiles and median values. Whiskers indicate the 5th and 95th percentile. Dashed lines indicate the chosen threshold values for the automated rock outcrop extraction and the values to be selected or discarded.

5

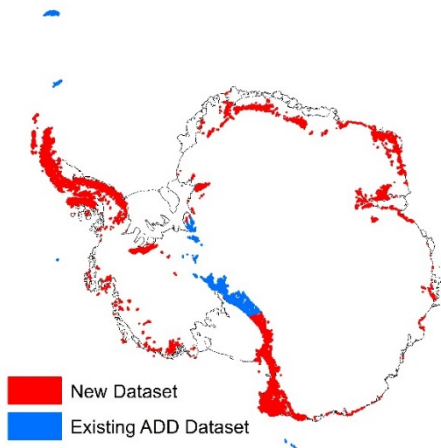


Fig. 6. Rock exposure map of Antarctica showing the data sources for the new dataset. Outcrops shown in red were derived using the new remote sensing methodology and outcrops in blue were derived from the existing ADD rock outcrop dataset to supplement areas south of 82°40' S (not covered by Landsat 8) or islands lacking suitable cloud free images. Areas of rock exposure are exaggerated for illustration.

10

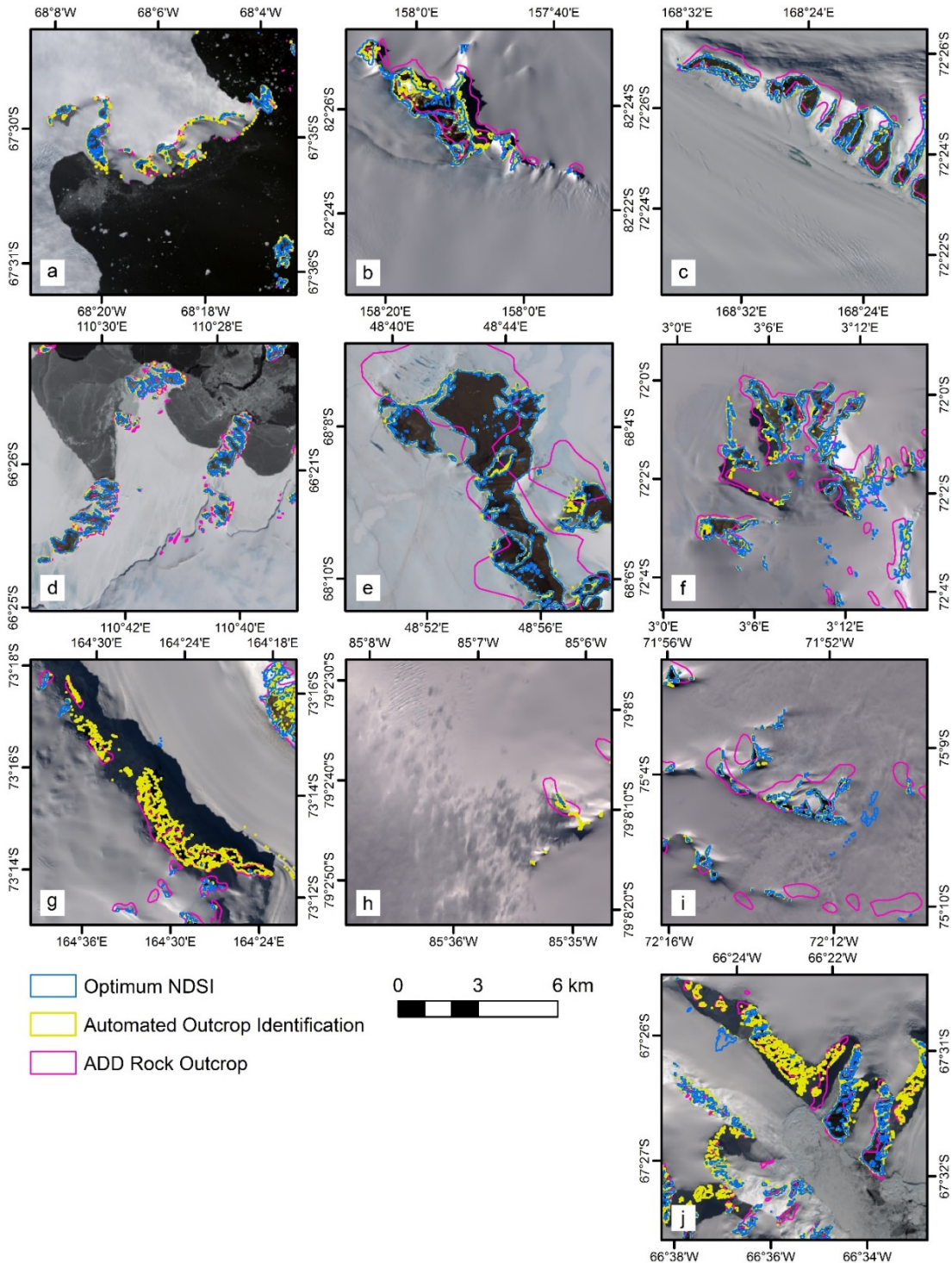
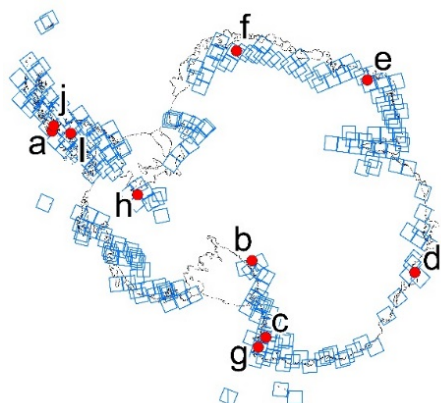


Fig. 7. Images used for the quality assessment overlain by the tree alternative methodologies and datasets: Pixels extracted using optimum NDSI thresholds for each image; pixels extracted using the new methodology presented here; and the extents of the current ADD rock outcrop map.



5 **Fig. 8.** Locations of the 249 Landsat 8 tiles (blue squares) used to identify rock outcrop in Antarctica and the locations (a to j) of the 10x10 km images used for the quality assessment in Fig. 5.

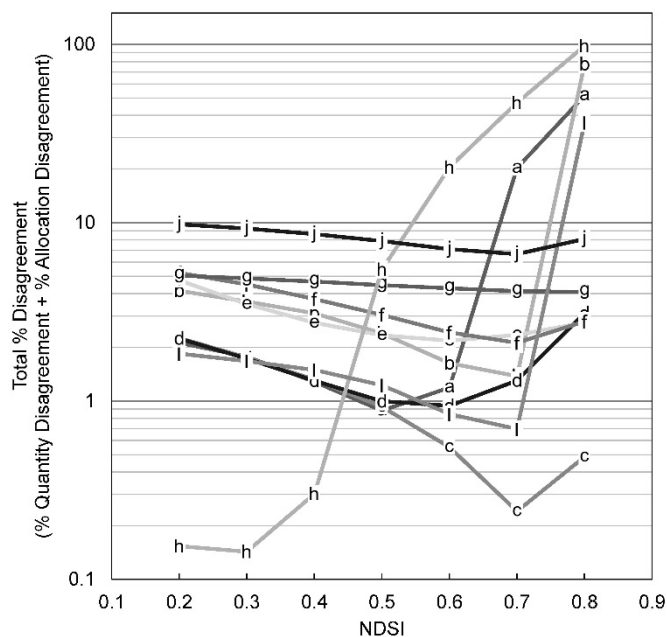


Fig. 9. Total quantity and allocation disagreement values (Pontius Jr and Millones, 2011) for pixels extracted from the images in Fig. 5 using the NDSI threshold technique.

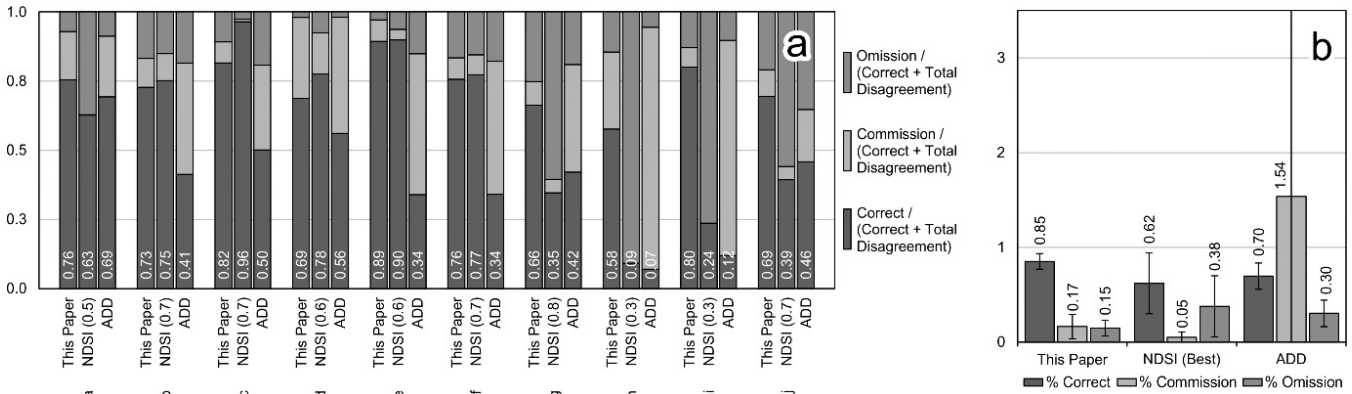


Fig. 10. (a) 100% normalised accuracy assessment data for correctly classified pixels and pixels of omission and commission disagreements for the images in Fig. 5. Optimal NDSI values used are shown in brackets. (b) Overall accuracy assessment data for the three alternative datasets. Error bars shown at 1SD.

5

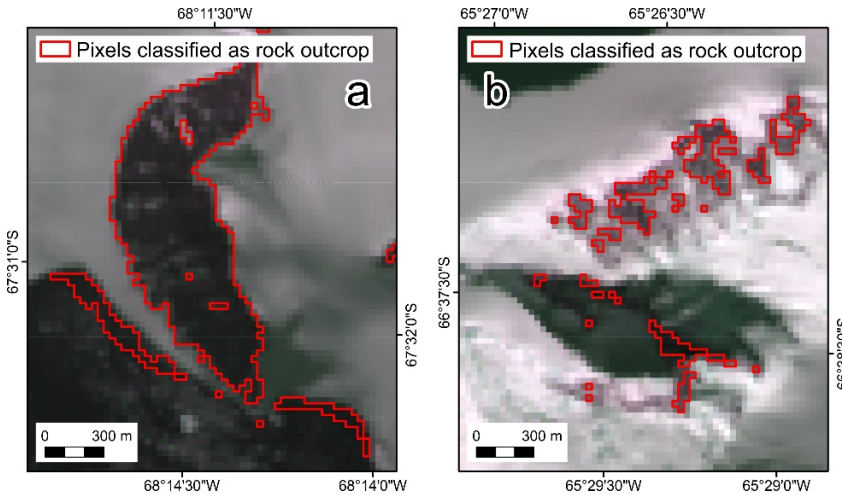


Fig. 11. Limitations of the new methodology. (a) Seawater near calving ice classified as rock (later removed manually). (b) An illustration of conservative outcrop extent estimation using the new technique.